ORIGINAL PAPER

Synthesis of graphene with both high nitrogen content and high surface area by annealing composite of graphene oxide and g-C_3N_4

Yurong Deng · Kewei Liu · Hongmei Cao · Mingliang Luo · Hongjian Yan

Abstract In this paper, we propose a facile, catalyst-free thermal annealing approach for synthesis of N-doping graphene (NG) using graphitic carbon nitride (g-C_3N_4) as the nitrogen source. Graphene with nitrogen content up to 13.9 % (atom %) and Brunauer–Emmett–Teller (BET) surface area of 419.6 m^2/g can be achieved via thermal annealing composite of graphene oxide (GO) and g-C_3N_4. The transmission electron microscopy indicates that the NG synthesized by annealing GO/g-C_3N_4 composite is compact and stacked with large sheets. The atomic force microscopy reveals that the NG was less than three single graphene layers nanosheets with an apparent thickness of about 1.0 nm. This improved synthesis method for producing high nitrogen content and high BET surface area can be extended to prepare multi-element (such as B and N) doping graphene nanosheets.

Keywords Carbon nitride · Graphite · Graphene · Graphene oxide · Nanomaterials

Introduction

Graphene, a novel nanomaterial of single-layer carbon atoms packed in a two-dimensional honeycomb lattice, has recently attracted wide-ranging interests because of its potential applications in nanoelectronics, energy conversion and storage materials, polymer composite materials, sensors, and catalysis [1–7]. Graphene has fascinating properties, such as high surface area, high thermal conductivity, fast charged carrier mobility and strong Young's modulus [8–10]. However, the application of the pristine graphene is limited by its gapless electronic structure. It is reported that the electron-donor properties of graphene can be tuned by controlling its morphology or chemical doping with foreign atoms, such as N, B, P, I and S, into the carbon lattice of graphene [11–14]. Both theoretical calculations and detailed experiments have proved that nitrogen doping has been an effective way to tailor the electronic properties and chemical reactivity of graphene [15–17].

To date, the NG can be obtained through direct synthesis way (such as chemical vapor deposition (CVD), segregation growth, solvothermal, or arc discharge approaches) [18–20] or post-treatment graphene oxide (GO) in the presence of appropriate nitrogen source (such as NH_3, N_2H_4, or nitrogen plasma) [21–24]. Compared with the direct synthesis way, the post-treatment method can avoid the metal catalysts remaining (such as nickel and copper) or using special instruments. Generally, the nitrogen content in the NG synthesized by the post-treatment way is relatively low. It was reported recently that NG with up to 10.1 % N content can be obtained via thermal annealing the mixture of GO and melamine [25]. However, the Brunauer–Emmett–Teller (BET) surface area of the NG synthesized by this method is as low as 6 m^2/g, much lower than that of pristine graphene (281 m^2/g) synthesized by annealing the GO alone. The low surface area may limit the catalytic application of the NG synthesized by this method because a low surface area provides less active sites for adsorption and catalytic reaction.

Herein, we report a facile approach for the synthesis of NG with both high nitrogen content and high surface area by thermal annealing composite of GO and g-C_3N_4.

Y. Deng · K. Liu · H. Cao · M. Luo · H. Yan (✉)
College of Chemistry, Sichuan University, Chengdu 610064,
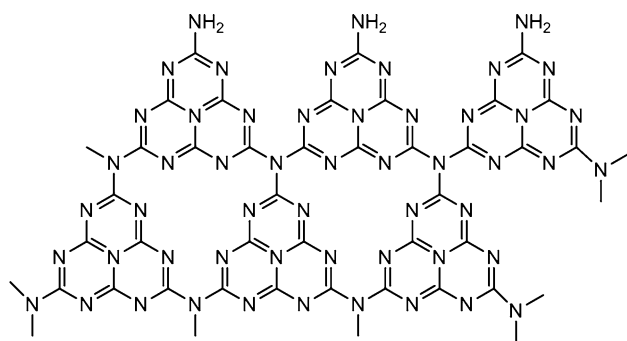People's Republic of China
e-mail: hjyan@scu.edu.cn

Fig. 1 The structure of g-C_3N_4

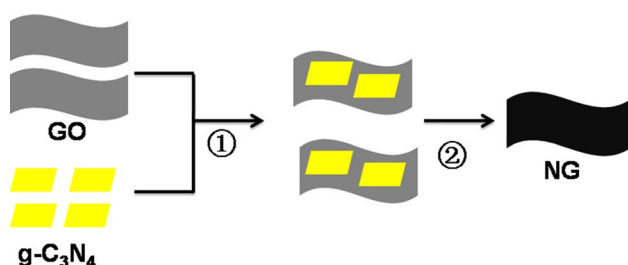**Fig. 2** Illustration of the nitrogen doping process by annealing the GO/g-C_3N_4 composite **a** sonication and mixed; **b** calcination at high temperature

The g-C_3N_4 has graphitic planes constructed from tri-s-triazine units connected by planar amino groups (Fig. 1) [26–32]. Furthermore, there are NH_2 groups still exist in the g-C_3N_4 [33, 34], which was confirmed by experimental IR and elemental analysis (EA) results. Thus, the g-C_3N_4 are favorable to be adsorbed on the surface of GO via hydrogen bonding force between terminal amino groups or bridging nitrogen atoms of g-C_3N_4 and OH, C–O–C or COOH groups of GO. During annealing, g-C_3N_4 decomposes into various nitrogen containing species, such as C_2N_2, $C_3N_2^+$ and $C_3N_3^+$, at temperatures over 600 °C [35]. These nitrogen containing species are nitrogen sources for synthesis of NG. Furthermore, the g-C_3N_4, absorbed on the surface of GO, can inhibit the restack of graphene sheets at high temperature. Thus, the high BET NG was obtained. The possible process is illustrated in Fig. 2. The EA and N_2 adsorption were employed to evaluate the nitrogen-doping degree and BET surface area of the NG sheets, respectively. It is found that graphene with nitrogen content up to 13.9 % (atom %) and BET surface area of 419.6 m^2/g can be obtained. To the best of our knowledge, this is the first time to report such phenomenon. The meaning of this work is not only to synthesize highly N-content graphene, but also provide a new idea for preparing high BET NG through catalyst-free route.

Experimental

Materials

Melamine, sulfuric acid (H_2SO_4) and triethanolamine were purchased from Chengdu Kelong Chemical Reagent Factory. Graphite flake was purchased from Sigma. Pluronic P123 was purchased from Aldrich. All reagents were used as received without further treatment.

Synthesis of GO

GO was prepared from graphite powder using an improved Hummers' method [36]. Typically, graphite flake (2.0 g) was added into a 9:1 mixture of concentrated H_2SO_4/H_3PO_4 (240:26 mL). Then, $KMnO_4$ (12.0 g) was added gradually under stirring. The mixture was then heated to 50 °C and stirred for 12 h. After cooled down to room temperature, the mixture was poured onto ice (300 mL) with 30 % H_2O_2 (3 mL). Then the mixture was centrifuged and washed with water (200 mL), HCl (30 % 200 mL) and ethanol (200 mL), successively. The obtained solid was vacuum-dried overnight at 45 °C.

Synthesis of g-C_3N_4

1. g-C_3N_4 with BET surface area of 8.6 m^2/g was synthesized by heating melamine at 600 °C for 4 h under a flow of Ar gas [37].
2. g-C_3N_4 with BET surface area of 15.6 m^2/g was synthesized by heating sulfuric acid-treated melamine at 600 °C for 4 h under a flow of Ar gas [38].
3. g-C_3N_4 with BET surface area of 90.3 m^2/g was synthesized via soft-templating method [39]. Typically, melamine (5.0 g) and Pluronic P123 (1.0 g) were dispersed in distilled water (100 mL) by heating at 100 °C for 1 h under reflux. White precipitate was produced by adding sulfuric acid solution (3 mL, H_2SO_4:H_2O = 1:1 in volume) to the solution. After cooling down to room temperature, the precipitate was collected by filtration, and then dried in an oven at 80 °C for overnight. The precipitate (3.0 g) was heated at 600 °C for 4 h under a flow of Ar gas. Finally, the product was then calcined at 500 °C for 2 h in air.

Synthesis of NG

GO and g-C_3N_4 were dispersed in ethanol separately for 1 h by sonication and then mixed together. After mixed, hybrid GO/g-C_3N_4 complex was obtained because of the low interface adhesion energy. Then the ethanol was removed by evaporation on water bath at 80 °C. After ethanol evaporation, the mixture was put into a quartz boat and

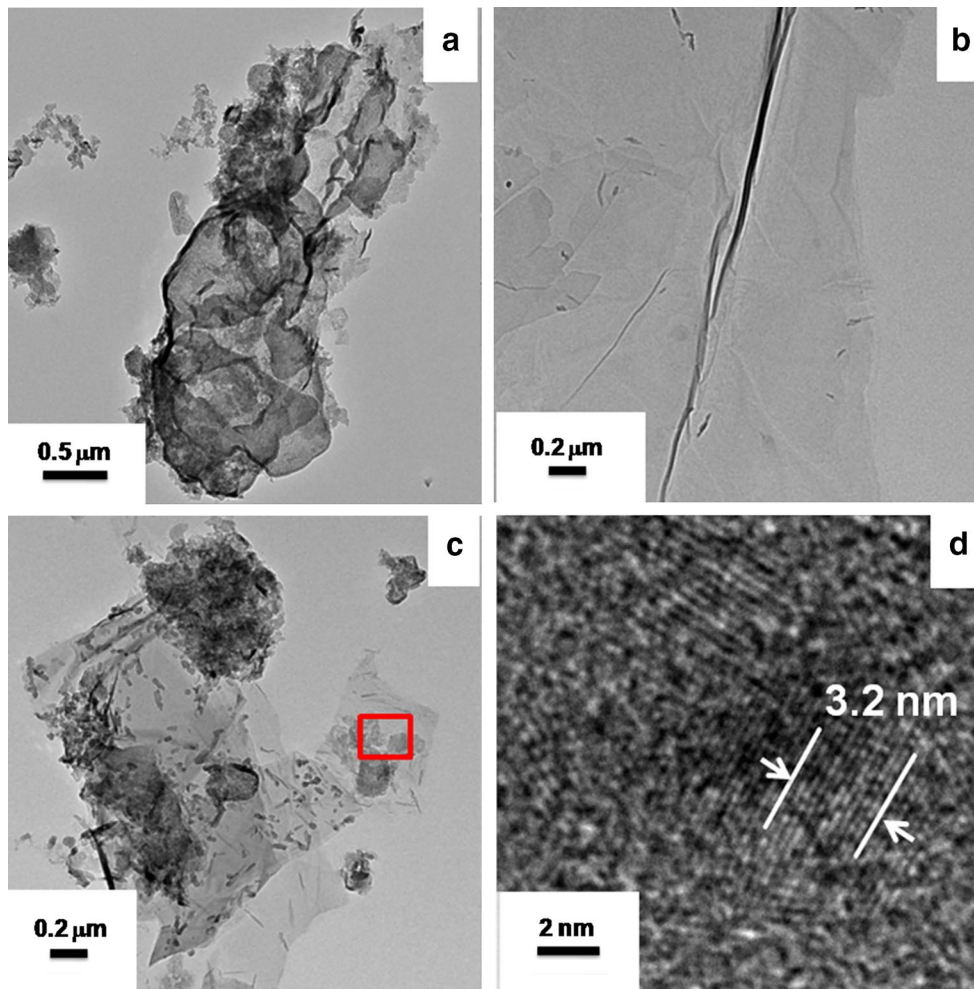**Fig. 3** TEM image of g-C_3N_4 (**a**), GO (**b**), and composite of g-C_3N_4 and GO (**c**). **d** the HRTEM of box marked in **c**
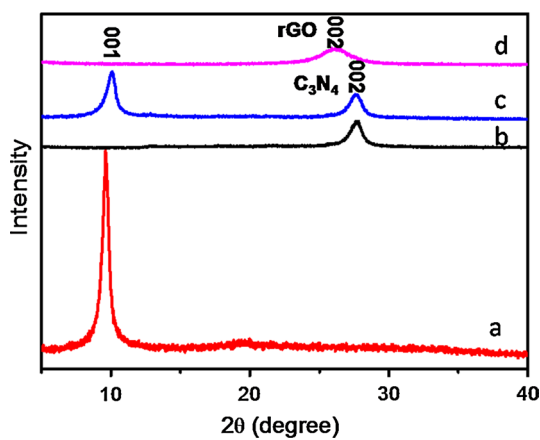
Fig. 4 The XRD patterns of GO (*a*), g-C_3N_4 (*b*), GO/g-C_3N_4 composite (*c*) and NG synthesized by annealing GO/g-C_3N_4 composite (*d*)
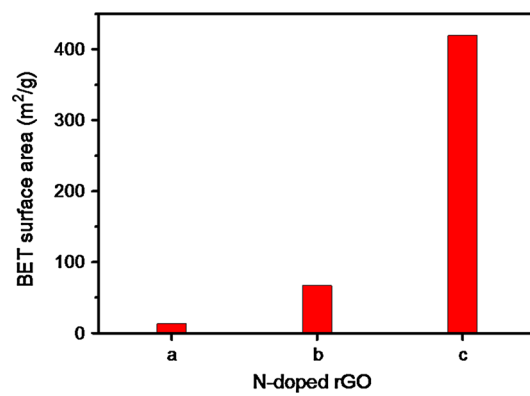

Fig. 5 BET surface area of NG synthesized by annealing the mixture of GO and melamine (*a*), the mixture of GO and melamine with sonication treatment (*b*), and the GO/g-C_3N_4 composite (*c*)

heated to 700 °C for 1 h in Ar flow. Then the furnace was cooled down to room temperature slowly. The final product was collected from the quartz boat directly.

Table 1 Elemental and BET results of NGs

Entry	Starting materials	C (atom %)	N (atom %)	BET (m²/g)
1	GO and melamine	82.5	10.7	13.1
2	GO and melamine[a]	81.7	12.4	50.0
3	GO and g-C₃N₄[b]	77.2	13.9	419.6
4	GO and g-C₃N₄[c]	80.3	13.1	369.1
5	GO and g-C₃N₄[d]	79.7	12.8	285.5

[a] GO and melamine was sonication for 1 h in ethanol (50 mL) before mixture, respectively

[b] g-C₃N₄ was synthesized via soft-templating method. The BET of g-C₃N₄ is 90.3 m²/g

[c] g-C₃N₄ was synthesized by heating sulfuric acid-treated melamine. The BET of g-C₃N₄ is 15.6 m²/g

[d] g-C₃N₄ was synthesized by heating melamine. The BET of g-C₃N₄ is 8.6 m²/g

The adsorption of methylene blue (MB) dye

The NGs (1.2 mg) were dispersed in 5 mL methylene blue (MB) solution (1.2×10^{-5} M). The samples were kept in the dark for 10 min. Then the samples were centrifuged to remove the NG. To study the change in absorbance maxima of the dye, the specific characteristic absorbance was measured by UV–vis absorbance spectroscopy (UV–vis 759, APL).

Characterization

EA was performed on a Euro EA3000 elemental analyser (Euro Vector S.P.A., Italy). X-ray diffraction (XRD) patterns were recorded on a X-Pert Pro diffractionmeter with Cu Kα radiation ($\lambda = 1.5406$ Å) at a scanning speed of 4° min⁻¹. The BET-specific surface areas were measured by N₂ adsorption at 77 K on a Quantachrome Instruments (Autosorb 1-C). The morphology of the composite
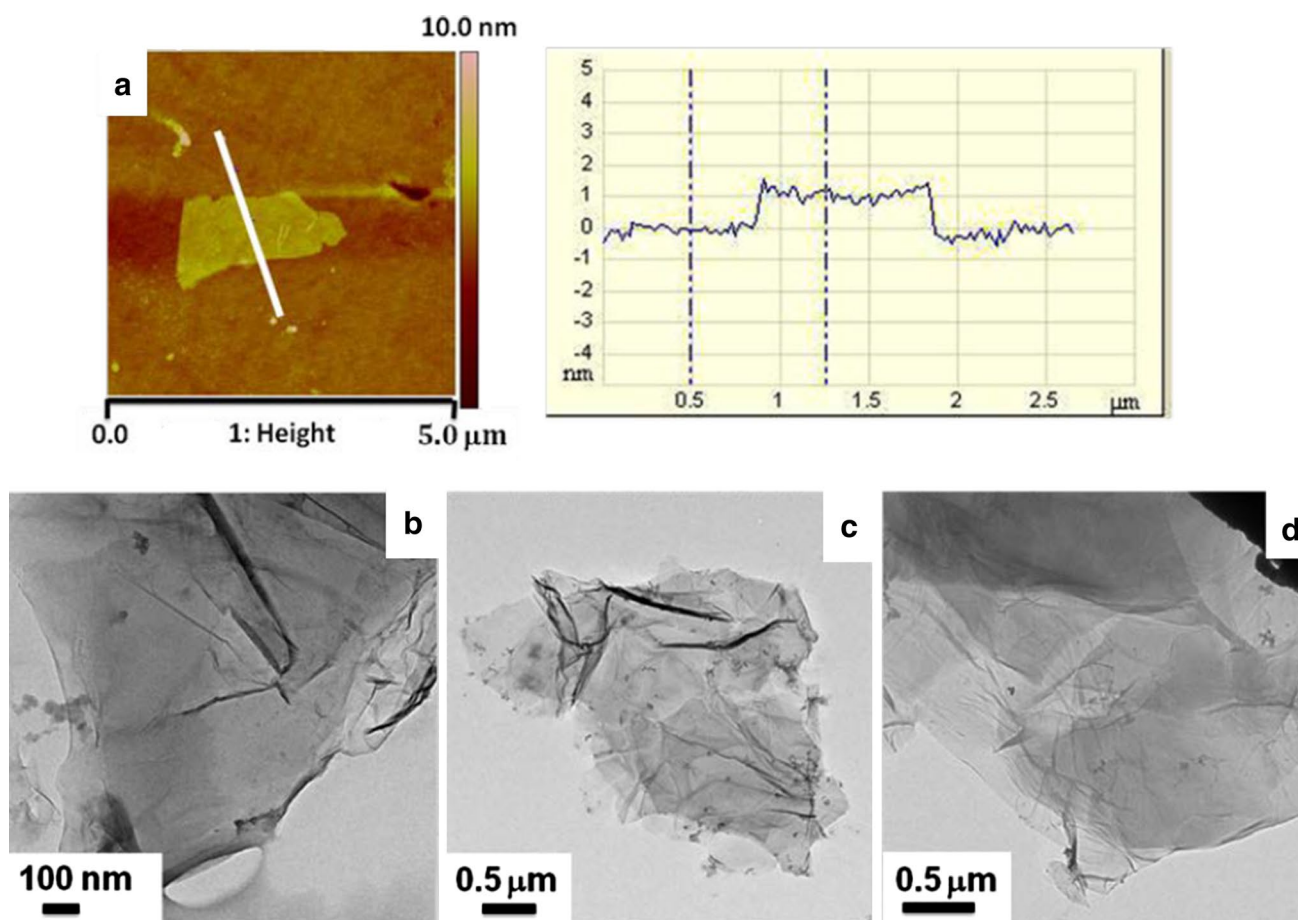

Fig. 6 **a** Typical AFM image of NG synthesized by annealing GO/g-C₃N₄ composite. **b** low-resolution TEM image of graphene synthesized by annealing GO without melamine or g-C₃N₄. **c** low-resolution TEM image of NG synthesized by annealing GO/g-C₃N₄ composite. **d** low-resolution TEM image NG synthesized by annealing the mixture of GO and melamine

materials was characterized using Tecnai G^2 F20 S-TWIN microscope.

Results and discussion

Transmission electron microscopy (TEM) was used to study the morphology and microstructures of g-C$_3$N$_4$, GO, and composite of g-C$_3$N$_4$ and GO. Figure 3a shows a typical TEM image of g-C$_3$N$_4$, which demonstrates that the g-C$_3$N$_4$ is layered and platelet like. As shown in Fig. 3b, GO has a two-dimensional structure consisting of compact and stacked sheets with micrometer-long wrinkles. It can be clearly observed from the TEM of the composite that some g-C$_3$N$_4$ are adsorbed on the surface of GO (Fig. 3c). The HRTEM image of the composite (Fig. 3d) exhibits fringes spacing of ca 0.32 nm, which correspond to the (002) plane of g-C$_3$N$_4$.

XRD patterns from the samples shown in Fig. 4 indicate that the composite presents a two-phase composition of g-C$_3$N$_4$ and GO. The GO's diffraction peak slightly shifts from 9.7° to 10.1°, due to the interaction of GO and

g-C$_3$N$_4$. After annealing, the diffraction peak of g-C$_3$N$_4$ at 27.8° disappears, and a broad peak at 26.4° corresponding to graphene appears. This result reveals that the g-C$_3$N$_4$ is decomposed and GO is reduced to graphene during annealing.

The BET-specific surface area of the as-synthesized NG was investigated by nitrogen adsorption. The BET of graphene, which was synthesized by thermal annealing GO without melamine or g-C$_3$N$_4$, is about 282.5 m^2/g. As shown in Fig. 5, the BET of NG obtained by annealing the mixture of GO and melamine, which were mixed by grinding, is 13.1 m^2/g, slightly higher than that of reported previously [25]. Sonication treatment of melamine before mixed with GO can increase the BET of NG about four times. However, the BET of NG obtained by annealing GO/g-C$_3$N$_4$ composite is 419.6 m^2/g, which is 31 times higher than that of NG obtained by annealing the mixture of GO and melamine. The resultants suggest that it is g-C$_3$N$_4$, not the sonication treatment before mixing, is responsible for the remarkable increase of NG's BET. It is believed that the nitrogen doping was accompanied by the elimination of epoxy and carboxyl groups. During the process
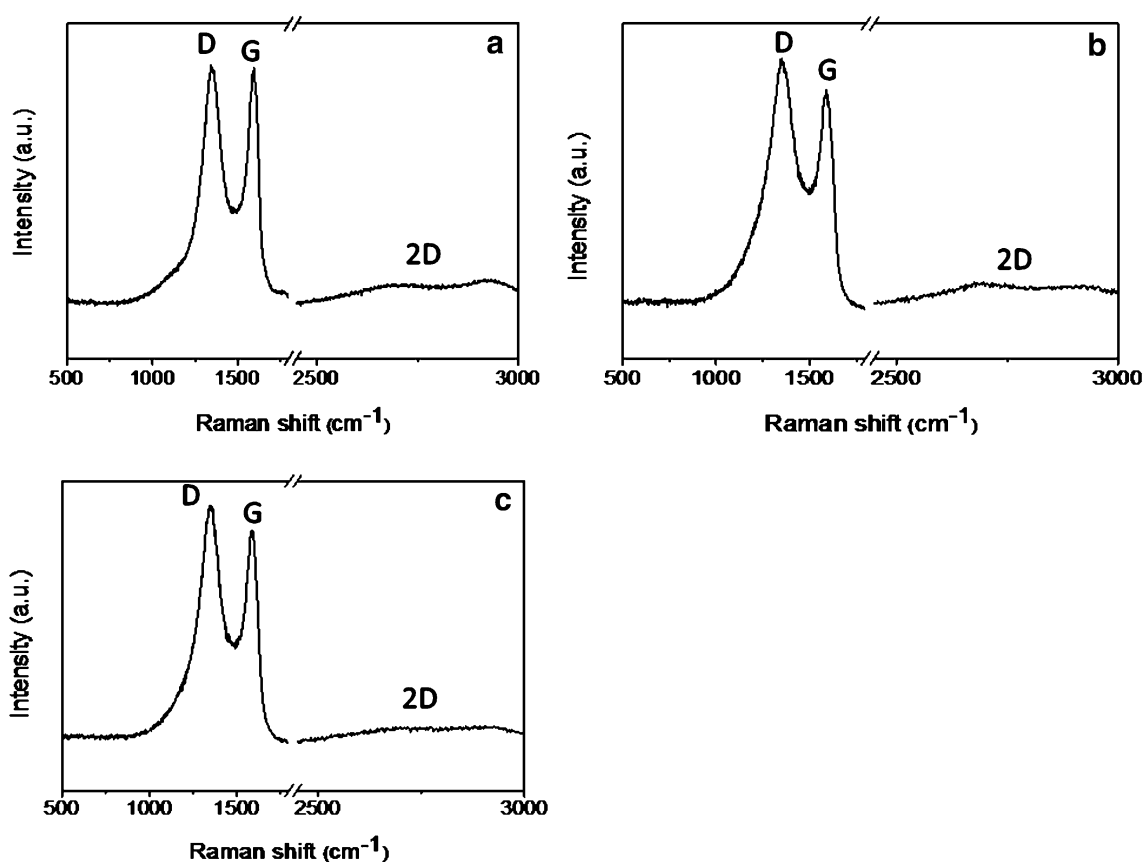

Fig. 7 The Raman spectra of GO (**a**), NG synthesized by annealing GO/g-C$_3$N$_4$ composite (**b**), and NG synthesized by annealing mixture of GO and melamine (**c**)

of thermal annealing, nitrogen atoms decomposed from melamine (or carbon nitride) attack the active sites which were released from the removal of oxygen groups linked to graphene nanosheets in GO to form NGs. However, within the temperature range from 180 to 600 °C, the interlayers for GO are contracted with the removal of the main carboxyl groups [40]. Meanwhile, melamine exhibits a strong tendency toward sublimation above 290 °C, which peaks around 345 °C [41]. Compared to melamine, however, g-C_3N_4 is thermally stable up to 600 °C [42], and therefore restrain the contraction of GO. Apart from the specific surface area being enhanced significantly, the nitrogen doping level of NG synthesized by annealing the GO/g-C_3N_4 composite increases slightly from 10.7 to 13.9 % (Table 1).

Figure 6a shows the typical AFM image of the exfoliated NG synthesized by annealing the GO/g-C_3N_4 composite. The NG is a nanosheet with an apparent thickness about 1.0 nm. The results reveal that the as-synthesized NG is less than three single graphene layers (considering that the theoretical thickness of a single-layer graphene is ~0.34 nm). As shown in Fig. 3b, GO is a two-dimensional nano sheet with micrometer-long wrinkles. The TEM indicate that the NGs synthesized by annealing GO without

melamine or g-C_3N_4, composite of GO and g-C_3N_4, and composite of GO and melamine are compact and stacked with large sheets (Fig. 6 b, c and d, respectively). More carbon particles (dark spot) exist on the surface of NG synthesized by annealing GO/g-C_3N_4. The similar morphology suggests that using g-C_3N_4 instead of melamine as N-source does not significantly change the morphology and texture of NG.

It was reported that the BET of g-C_3N_4 can be tuned by changing the synthesis method [37–39]. To investigate the influence of surface area of g-C_3N_4 on the NG's BET, three g-C_3N_4 with different BET surface area (8.6, 15.6, and 90.3 m^2/g) were mixed with GO, respectively. The results shown in Table 1 indicate that the BET of NG increases with the BET of g-C_3N_4. The higher BET of NG obtained using g-C_3N_4 with higher surface area may be ascribed to the fact that g-C_3N_4 with higher BET can well dispersed on the surface of GO.

For nitrogen doping, the substitution of nitrogen atoms is usually accompanied with the introduction of defects into the graphene surface. Therefore, Raman spectroscopy was used to characterize the structure and quality of NGs, including the defects. As shown in Fig. 7, two remarkable
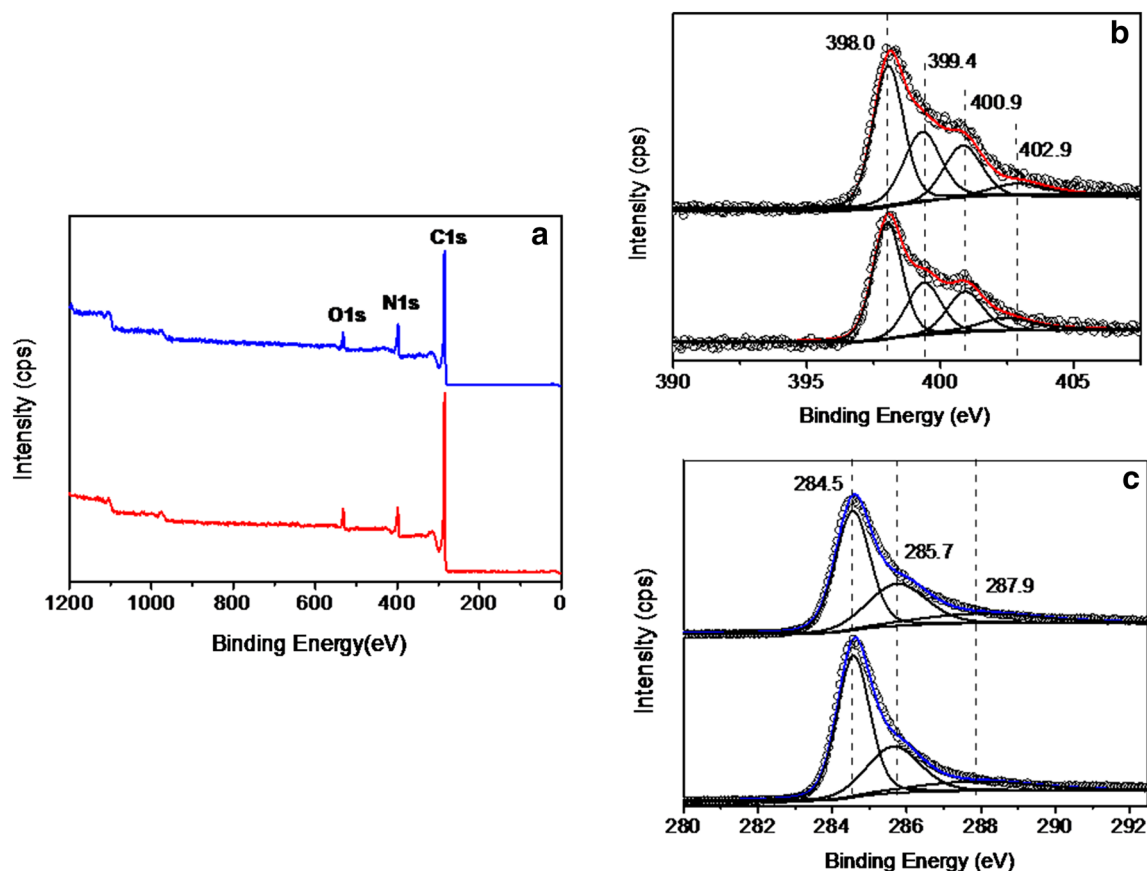

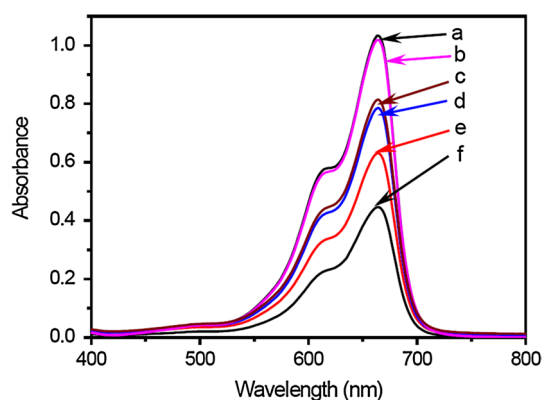**Fig. 8** XPS of NG from GO/g-C_3N_4 (*up*) and NG from GO/melamine (*down*). **a** wide scan, **b** N 1 s, and **c** C 1 s

Fig. 9 The UV–vis spectra of MB solution (1.2×10^{-5} M) before adsorption (*a*), and after adsorption by NGs. The BET surface area of sample *b*, *c*, *d*, *e*, and *f* is 13.1, 282.5, 285.5, 369.1, and 419.6 m^2/g, respectively

peaks at ~1,345 and ~1,590 cm^{-1} attributing to the well-defined D band and G band, respectively, can be observed. The I_D/I_G values for GO is ~1.02. The I_D/I_G values for NG synthesized by annealing GO/g-C$_3$N$_4$ (ca 1.12) are the same as that of NG synthesized by annealing GO/melamine (1.14). This indicates that using g-C$_3$N$_4$ as N-source does not significantly change the defects of NG.

X-ray photoelectron spectroscopy (XPS) was performed to detect the elemental composition and nitrogen bonding configurations in NGs as shown in Fig. 8. The XPS spectra for NG (Fig. 8a) clearly show the incorporation of nitrogen atoms within the graphene sheets. The high-resolution N1 s spectrum can be deconvoluted to four individual peaks located at 398.0, 399.4, 400.9, 402.9 eV, which were assigned to pyridinic N, pyrrolic N, quaternary N (graphitic N) and oxidized N [25], respectively. The dominant component of N1 s spectra-pyridinic N is sp^2 hybridized. The pyrrolic N is sp^3 hybridized, often occurring and being located in the defect or the boundary of the graphene. Quaternary N refers to nitrogen incorporated into the graphene network as graphitic N by substitution for carbon atoms in the hexagonal ring. As shown by the N1 s spectra, the intensity of pyridinic N is much higher than those of other nitrogen types. Pyrrolic N and graphitic N are the secondary main components of N1 s, their intensities are almost the half that of pyridinic N. XPS spectra are very similar with each other for the two NGs from the mixture of GO and melamine and GO and g-C$_3$N$_4$.

To evaluate the performance of NGs, the adsorption of MB dye was carried out. As shown in Fig. 9, all the samples show the property for the adsorption of MB. The adsorption amount of MB on NGs increases with the increase of BET surface area of NGs. The adsorption amount of MB on NG with BET of 13.1 m^2/g, which was synthesized by thermal annealing GO and melamine, is about 2.3 %. However, the adsorption amount of MB on NG with BET of 419.6 m^2/g, which was synthesized by thermal annealing GO and g-C$_3$N$_4$, achieves 56.8 %. These results indicate that the NG with high BET surface area synthesized by annealing the composite of GO and g-C$_3$N$_4$ is a promising material for pollutant adsorption.

Conclusions

N-doped graphene has been synthesized via a facile, catalyst-free thermal annealing approach using g-C$_3$N$_4$ as the nitrogen source. The resultant NG has high nitrogen content up to 13.9 %, as well as much higher surface area up to 419.6 m^2/g than those of reported. The NG was less than three single graphene layers nanosheets with an apparent thickness about 1.0 nm. This improved synthesis method for producing high nitrogen content and high BET surface area can be extended to prepare multi-element (such as B and N) doping graphene nanosheets.

References

1. H. Wang, T. Maiyalagan, X. Wang, Review on recent progress in nitrogen-doped graphene: synthesis, characterization, and its potential applications. ACS Catal. **2**, 781–794 (2012)
2. M.J. Allen, V.C. Tung, R.B. Kaner, Honeycomb carbon: a review of graphene. Chem. Rev. **110**, 132–145 (2010)
3. M.D. Stoller, S.J. Park, Y.W. Zhu, J.H. An, R.S. Ruoff, Graphene-based ultracapacitors. Nano Lett. **8**, 3498–3502 (2008)
4. S. Stankovich, D.A. Dikin, G.H.B. Dommett, K.M. Kohlhaas, E.J. Zimney, E.A. Stach, R.D. Piner, S.T. Nguyen, R.S. Ruoff, Graphene-based composite materials. Nature **442**, 282–286 (2006)
5. A.V. Murugan, T. Muraliganth, A. Manthiram, Rapid, facile microwave-solvothermal synthesis of graphene nanosheets and their polyaniline nanocomposites for energy strorage. Chem. Mater. **21**, 5004–5006 (2009)
6. C.H. Lu, H.H. Yang, C.L. Zhu, X. Chen, G.N. Chen, A graphene platform for sensing biomolecules. Angew. Chem. Int. Ed. **48**, 4785–4787 (2009)
7. E.J. Yoo, J. Kim, E. Hosono, H.S. Zhou, T. Kudo, I. Honma, Large reversible Li storage of graphene nanosheet families for use in rechargeable lithium ion batteries. Nano Lett. **8**, 2277–2282 (2008)
8. A.K. Geim, K.S. Novoselov, The rise of graphene. Nat. Mater. **6**, 183–191 (2007)
9. A.A. Balandin, S. Ghosh, W. Bao, I. Calizo, D. Teweldebrhan, F. Miao, C.N. Lau, Superior thermal conductivity of single-layer graphene. Nano Lett. **8**, 902–907 (2008)
10. C. Lee, X. Wei, J.W. Kysar, J. Hone, Measurement of the elastic properties and intrinsic strength of monolayer graphene. Science **321**, 385–388 (2008)
11. L. Qu, Y. Liu, J. Baek, L. Dai, Nitrogen-doped graphene as efficient metal-free electrocatalyst for oxygen reduction in fuel cells. ACS Nano **4**, 1321–1326 (2010)

12. Z. Liu, F. Peng, H. Wang, H. Yu, W. Zheng, J. Yang, Phosphorus-doped graphite layers with high electrocatalytic activity for the O_2 reduction in an alkaline medium. Angew. Chem. Int. Ed. **50**, 3257–3261 (2011)

13. Z. Yao, H. Nie, Z. Yang, X. Zhou, Z. Liu, S. Huang, Catalyst-free synthesis of iodine-doped graphenevia a facile thermal annealing process and its use for electrocatalytic oxygen reduction in an alkaline medium. Chem. Commun. **48**, 1027–1029 (2012)

14. Z. Yang, Z. Yao, G. Li, G. Fang, H. Nie, Z. Liu, X. Zhou, X. Chen, S. Huang, Sulfur-doped graphene as an efficient metal-free cathode catalyst for oxygen reduction. ACS Nano **6**, 205–211 (2012)

15. Y.F. Li, Z. Zhou, P.W. Shen, Z.F. Chen, Spin gapless semiconductor–metal–half-metal properties in nitrogen-doped zigzag graphene nanoribbons. ACS Nano **3**, 1952–1958 (2009)

16. M. Deifallah, P.F. McMillan, F.J. Cora, Electronic and structural properties of two-dimensional carbon nitride graphenes. Phys. Chem. C **112**, 5447–5453 (2008)

17. Y.Z. Xue, B. Wu, L. Jiang, Y.L. Guo, L.P. Huang, J.Y. Chen, J.H. Tan, D.C. Geng, B.L. Luo, W.P. Hu, G. Yu, Y.Q. Liu, Low temperature growth of highly nitrogen-doped single crystal graphene arrays by chemical vapor deposition. J. Am. Chem. Soc. **134**, 11060–11063 (2012)

18. D.C. Wei, Y.Q. Liu, Y. Wang, H.L. Zhang, L.P. Huang, G. Yu, Synthesis of N-doped graphene by chemical vapor deposition and its electrical properties. Nano Lett. **9**, 1752–1758 (2009)

19. D.H. Deng, X.L. Pan, L. Yu, Y. Cui, Y.P. Jiang, J. Qi, W.X. Li, Q. Fu, X.C. Ma, Q.K. Xue, G.Q. Sun, X.H. Bao, Toward N-doped graphene via solvothermal synthesis. Chem. Mater. **23**, 1188–1193 (2011)

20. L.S. Panchakarla, K.S. Subrahmanyam, S.K. Saha, A. Govindaraj, H.R. Krishnamurthy, U.V. Waghmare, C.N.R. Rao, Synthesis structure and properties of boron- and nitrogen-doped graphene. Adv. Mater. **21**, 4726–4730 (2009)

21. X.R. Wang, X.L. Li, L. Zhang, Y.K. Yoon, P.K. Weber, H.L. Wang, J. Guo, H.J. Dai, N-doping of graphene through electrothermal reactions with ammonia. Science **324**, 768–771 (2009)

22. Y. Wang, Y.Y. Shao, D.W. Matson, J.H. Li, Y.H. Lin, Nitrogen-doped graphene and its application in electrochemical biosensing. ACS Nano **4**, 1790–1798 (2010)

23. Y.Y. Shao, S. Zhang, M.H. Engelhard, G.S. Li, G.C. Shao, Y. Wang, J. Liu, I.A. Aksay, Y.H. Lin, Nitrogen-doped graphene and its electrochemical applications. J. Mater. Chem. **20**, 7491–7496 (2010)

24. X.L. Li, H.L. Wang, J.T. Robinson, H. Sanchez, G. Diankov, H.J. Dai, Simultaneous nitrogen doping and reduction of graphene oxide. J. Am. Chem. Soc. **31**, 15939–15944 (2009)

25. Z.H. Sheng, L. Shao, J.J. Chen, W.J. Bao, F.B. Wang, X.H. Xia, Catalyst-free synthesis of nitrogen-doped graphene via thermal annealing graphite oxide with melamine and its excellent electrocatalysis. ACS Nano **5**, 4350–4358 (2011)

26. X.C. Wang, K. Maeda, A. Thomas, K. Takanabe, G. Xin, J.M. Carlsson, K. Domen, M. Antonietti, A metal-free polymeric photocatalyst for hydrogen production from water under visible light. Nat. Mater. **8**, 76–80 (2009)

27. X.C. Wang, X.F. Chen, A. Thomas, X.Z. Fu, M. Antonietti, Metal-containing carbon nitride compounds: a new functional organic–metal hybrid material. Adv. Mater. **21**, 1609–1612 (2009)

28. Y.J. Zhang, T. Mori, J.H. Ye, M. Antonietti, Phosphorus-doped carbon nitride solid: enhanced electrical conductivity and photocurrent generation. J. Am. Chem. Soc. **132**, 6294–6295 (2010)

29. J.S. Zhang, X.F. Chen, K. Takanabe, K. Maeda, K. Domen, J.D. Epping, X.Z. Fu, M. Antonietti, X.C. Wang, Synthesis of a carbon nitride structure for visible-light catalysis by copolymerization. Angew. Chem. Int. Ed. **49**, 441–444 (2010)

30. Y.J. Zhang, A. Thomas, M. Antonietti, X.C. Wang, Activation of carbon nitride solids by protonation: morphology changes, enhanced ionic conductivity, and photoconduction experiments. J. Am. Chem. Soc. **131**, 50–51 (2009)

31. X.C. Wang, K. Maeda, X.F. Chen, K. Takanabe, K. Domen, Y.D. Hou, X.Z. Fu, M. Antonietti, Polymer semiconductors for artificial photosynthesis: hydrogen evolution by mesoporous graphitic carbon nitride with visible light. J. Am. Chem. Soc. **131**, 1680–1681 (2009)

32. X.F. Chen, J.S. Zhang, X.Z. Fu, M. Antonietti, X.C. Wang, Fe–g-C_3N_4-catalyzed oxidation of benzene to phenol using hydrogen peroxide and visible light. J. Am. Chem. Soc. **131**, 11658–11659 (2009)

33. Y. Guo, S. Chu, S.C. Yan, Y. Wang, Z.G. Zou, Developing a polymeric semiconductor photocatalyst with visible light response. Chem. Commun. **46**, 7325–7327 (2010)

34. M.J. Bojdys, J.O. Müller, M. Antonietti, A. Thomas, Ionothermal synthesis of crystalline, condensed, graphitic carbon nitride. Chem. Eur. J. **14**, 8177–8182 (2008)

35. H.Z. Zhao, M. Lei, X.A. Yang, J.K. Jian, X.L. Chen, Route to GaN and VN assisted by carbothermal reduction process. J. Am. Chem. Soc. **127**, 15722–15723 (2005)

36. D.C. Marcano, D.V. Kosynkin, J.M. Berlin, A. Sinitskii, Z.Z. Sun, A. Slesarev, L.B. Alemany, W. Lu, J.M. Tour, Improved synthesis of graphene oxide. ACS Nano **4**, 4806–4814 (2010)

37. H.J. Yan, H.X. Yang, TiO_2–g-C_3N_4 composite materials for photocatalytic H_2 evolution under visible light irradiation. J. Alloys Compd. **509**, L26–L29 (2011)

38. H.J. Yan, Y. Chen, S.M. Xu, Synthesis of graphitic carbon nitride by directly heating sulfuric acid treated melamine for enhanced photocatalytic H_2 production from water under visible light. Int. J. Hydrogen Energy **37**, 125–133 (2012)

39. H.J. Yan, Soft-templating synthesis of mesoporous graphitic carbon nitride with enhanced photocatalytic H_2 evolution under visible light. Chem. Commun. **48**, 3430–3432 (2012)

40. S.H. Huh, in Physics and Applications of Graphene—Experiments, ed. by S. Mikhailov (InTech, New York, 2011)

41. A. Thomas, A. Fischer, F. Goettmann, M. Antonietti, J. Muller, R. Schlogl, J.M. Carlsson, Graphitic carbon nitride materials: variation of structure and morphology and their use as metal-free catalysts. J. Chem. Mater. **18**, 4893–4908 (2008)

42. S.C. Yan, Z.S. Li, Z.G. Zou, Photodegradation performance of g-C_3N_4 fabricated by directly heating melamine. Langmuir **25**, 10397–10401 (2009)